

DOI: 10.1002/cssc.201300263

Dehydrogenation of Dodecahydro-*N*-ethylcarbazole on Pt(111)

Christoph Gleichweit,^[a] Max Amende,^[a] Stefan Schernich,^[a] Wei Zhao,^[a]
Michael P. A. Lorenz,^[a] Oliver Höfert,^[a] Nicole Brückner,^[b] Peter Wasserscheid,^[b, c]
Jörg Libuda,^[a, c] Hans-Peter Steinrück,^[a, c] and Christian Papp^{*[a]}

In the coming decades, the use of renewable energy sources will become unavoidable, both to reduce CO₂ emissions for climate reasons and to compensate for declining fossil-fuel resources. Electric energy will mainly be produced from wind or solar power plants. Due to its dependence on weather conditions, energy availability and demand will be often in a mismatch time- and location-wise. As a consequence, efficient energy storage and distribution systems are required. Presently, the most-discussed concepts are the extension of electric grids and the use of batteries. The first "solution" only improves energy distribution, but not the storage, and the second is only suitable for short-term storage cycles. For long-term energy storage (e.g., to compensate for seasonal changes) or for long-distance energy transport (e.g., to bring regenerative geothermal energy from Iceland to Western Europe) chemical energy storage systems are needed. In this context the use of hydrogen or of hydrogen-carrying chemicals is most promising.^[1–3]

The gravimetric energy storage density of H₂ is excellent (33 kWh kg⁻¹). This is in sharp contrast, however, to the volumetric energy storage density, which is only 3 Wh per liter of gaseous H₂ under ambient pressure. In existing technical applications H₂ is, therefore, either stored in its gaseous state under very high pressures (up to 700 bar) or in the liquid state (at –253 °C). Both scenarios are unfavorable for large-scale practical use and complicate storage, transport, and distribution technologies of molecular H₂. Reforming of hydrocarbons or alcohols and the application of metal hydrides have also been proposed as possible storage technologies.^[4,5] However, reforming suffers from a high CO content of the hydrogen gas flow, which poses a problem for fuel cells; in case of methanol,

its toxicity might not allow for large-scale applications. For metal hydrides the storage capacity is generally low, and for mixed metal hydrides side reactions can be a serious problem. One possible solution is "chemical storage" by using liquid organic hydrogen carrier (LOHC) materials.^[6,7] LOHCs are high-boiling organic molecules, which can be easily and reversibly hydrogenated and dehydrogenated in catalytic processes. One of the promising candidates is *N*-ethylcarbazole (NEC), which can be hydrogenated over supported Ru catalysts to dodecahydro-*N*-ethylcarbazole (H₁₂-NEC). In this process, 6 mol H₂ per mol NEC are added to the NEC starting material, yielding a H₂ storage capacity of 5.8 wt% in H₁₂-NEC.^[8,9] H₁₂-NEC is, in a number of practically relevant physicochemical properties (vapor pressure, flammability, viscosity), similar to today's commonly used diesel fuel. Consequently, the infrastructure for liquid fuels (such as for example, storage tanks, tank ships, filling stations) is in principal also useable for storage, transport, and distribution of LOHCs. Dehydrogenation of H₁₂-NEC is typically catalyzed by supported Pt or Pd catalysts.^[10–13] The dehydrogenation product NEC can be rehydrogenated in a sustainable, cyclic process allowing its application as recyclable hydrogen carrier.

Presently, the details of the dehydrogenation reaction from H₁₂-NEC to NEC are not fully understood. First efforts to study this reaction under model conditions have been undertaken on Pd particles.^[14] However, the size of the molecules (with, for example, 40 atoms in the case of H₁₂-NEC) makes these LOHC systems difficult to address by means of surface science methods. Furthermore, most spectroscopic properties are unknown, especially when adsorbed on surfaces. Thus, these systems represent a major challenge for detailed surface science and model catalytic studies, which have proven to work well for much smaller molecules such as hydrocarbons up to the size of benzene and with high symmetry; for examples, see References [15–17].

Herein, we present an in situ study of H₁₂-NEC on a Pt(111) single-crystal surface as model for the (111) facets of real catalyst particles and address the mechanism of dehydrogenation and side reactions on the molecular scale. We demonstrate that synchrotron radiation-based in situ high resolution X-ray photoelectron spectroscopy (HR-XPS) is an excellent method to investigate the thermally induced dehydrogenation, dealkylation, and decomposition of H₁₂-NEC. These reactions can be followed in great detail through careful and quantitative analysis, and individual reaction steps can be identified. These include the desired dehydrogenation of H₁₂-NEC to NEC, but also

[a] C. Gleichweit, M. Amende, S. Schernich, W. Zhao, M. P. A. Lorenz, O. Höfert, Prof. J. Libuda, Prof. H.-P. Steinrück, Dr. C. Papp
Lehrstuhl für Physikalische Chemie II
Friedrich-Alexander-Universität Erlangen-Nürnberg
Egerlandstrasse 3, 91058 Erlangen (Germany)
E-mail: christian.papp@chemie.uni-erlangen.de

[b] N. Brückner, Prof. P. Wasserscheid
Lehrstuhl für Chemische Reaktionstechnik
Friedrich-Alexander-Universität Erlangen-Nürnberg
Egerlandstrasse 3, 91058 Erlangen (Germany)

[c] Prof. P. Wasserscheid, Prof. J. Libuda, Prof. H.-P. Steinrück
Erlangen Catalysis Resource Center
Friedrich-Alexander-Universität Erlangen-Nürnberg
Egerlandstr. 3, 91058 Erlangen (Germany)

 Supporting Information for this article is available on the WWW under <http://dx.doi.org/10.1002/cssc.201300263>.

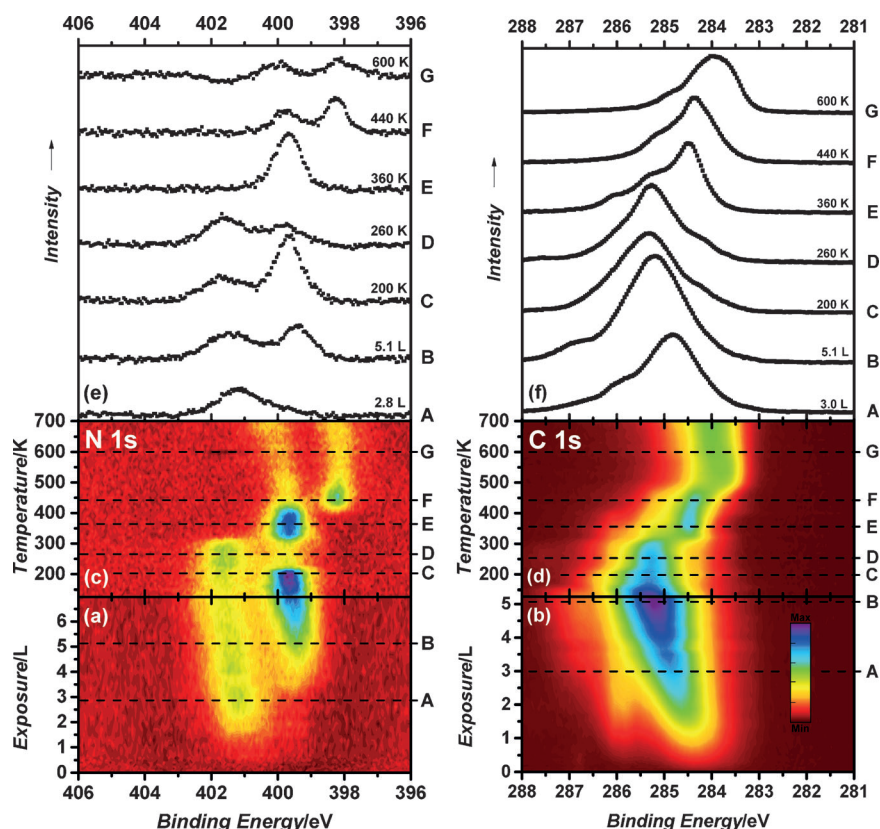


Figure 1. XP spectra of adsorption and reaction of H_{12} -NEC on Pt(111); on the left hand side in (a) and (c) the N 1s spectra of the adsorption and reaction of H_{12} -NEC, and on the right hand side in (b) and (d) the respective C 1s spectra are shown as a color-coded density plot. The lines in (a)–(d) indicate the temperatures/exposures of the spectra shown in the upper panels (e) and (f).

the unwanted dealkylation of NEC to carbazole and the formation of elemental carbon on the surface. Controlling the latter two processes is important to prevent loss of NEC in the storage cycle and catalyst deactivation.

At first we address the adsorption of the hydrogen-loaded H_{12} -NEC molecule on Pt(111) at 140 K, which is the starting point of the subsequent unloading of hydrogen, that is, the dehydrogenation reaction. Both, the N 1s and C 1s regions were measured continuously during exposure to H_{12} -NEC; selected individual spectra are shown in Figure 1 e and f, and the respective complete data sets are depicted in color-coded density plots in Figure 1 a and b. Molecular adsorption is verified by the growing peaks at 401.3 eV in the N 1s region and at 284.5 eV in the C 1s region at 2 langmuir (L). At higher exposures, the C 1s peak increases in width and shifts towards higher binding energies, whereas in the N 1s region a second signal develops at approximately 399.5 eV. These changes are attributed to the formation of the second H_{12} -NEC layer (and further layers, subsequently). The layer-wise growth is in line with previous studies on small molecules.^[15,18]

The quantitative nature of XPS allows us to determine the surface coverage from the N 1s and C 1s spectra as a function of exposure, as shown in Figure 2 a and b, respectively. The completed first H_{12} -NEC layer (monolayer) corresponds to approximately 0.07 monolayers (ML) (molecules per substrate atom) or approximately 1.0 C atom per Pt atom on the surface.

The small differences between the coverage values as derived from the N 1s and the C 1s regions arise from differences in photoelectron diffraction at the low kinetic energy of the photoelectrons (≈ 100 eV).

Next, the thermal evolution of the adsorbed H_{12} -NEC layer is followed by temperature-programmed XPS (TPXPS), that is, by heating the sample with a constant rate of 0.5 K s^{-1} while continuously measuring XP spectra. Selected N 1s and C 1s spectra are shown in Figure 1 e and f, the color-coded density plots of the full data sets in Figure 1 c and d, and the corresponding quantitative analyses in Figure 2 c and d, respectively. The starting point of these experiments is the end point of the adsorption experiment shown in Figure 1 a and b. The difference between the end of the adsorption experiment and the beginning of the heating experiment in the N 1s region is due to postadsorption of H_{12} -NEC after closing the valve.

As the N 1s and the C 1s spectra were obtained in independent

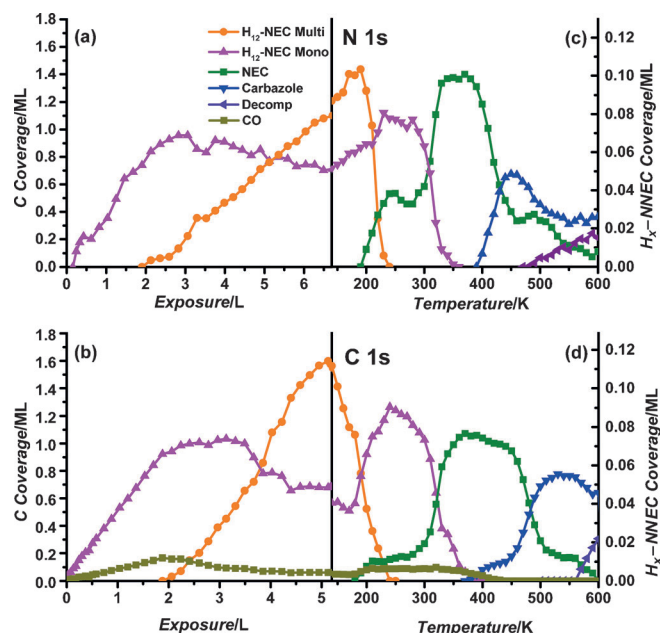


Figure 2. Quantitative analysis of the XPS experiments with H_{12} -NEC shown in Figure 1. In (a) and (c) the analysis of the N 1s spectra of the adsorption and reaction, and in (b) and (d) the respective analysis of the C 1s region are shown.

experiments, also the final coverage achieved after adsorption (and thus before the TPXPS measurement) is not identical, leading to a slightly different damping, that is, intensity loss of the monolayer by the multilayer on top of it. The small differences in the coverage of different intermediates in the quantitative analysis in Figure 2 are assigned to photoelectron diffraction, and/or uncertainties in the peak fitting, in particular in the C 1s region.

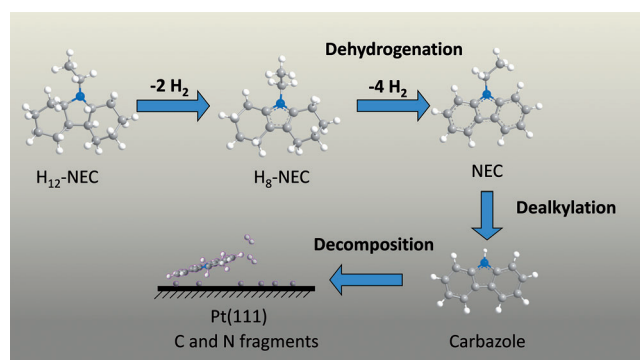
In the N 1s region, shown in Figure 1c, a pronounced decrease of the peak at 399.5 eV is observed up to 240 K, indicating desorption of the physisorbed H₁₂-NEC multilayer. Simultaneously, the peak of the H₁₂-NEC monolayer at 401.6 eV increases, due to reduced damping by the multilayer on top. In the C 1s region, shown in Figure 1d, the broad peak due to the multilayer/monolayer centered at 285.3 eV decreases in height and width and slightly shifts to lower binding energy (285.2 eV) due to desorption of the H₁₂-NEC multilayer. The remaining monolayer intensity has also increased in height due to the reduced damping.

Starting at 200 K, new N 1s and C 1s peaks develop at 399.5 and 284.5 eV, respectively, indicating the beginning of the dehydrogenation of H₁₂-NEC (note that the N 1s peak has the same binding energy as the multilayer peak, and consequently the separation is somewhat ambiguous in the transition region between 200 and 260 K). At 300 K, these peaks start to strongly increase at the cost of the H₁₂-NEC monolayer peaks at 401.6 and 285.2 eV, respectively. The large binding energy difference of 2.1 eV for the N 1s peak, as compared to 0.7 eV for the C 1s peak, suggests that the initial dehydrogenation is accompanied by a major change of the bonding of the nitrogen atom to the surface. This is in line with a previously suggested reaction mechanism on Pd, in which the first dehydrogenation occurs at the carbon atoms next to the nitrogen atom, that is, the α -carbon atoms of the pyrrole ring.^[13,14] Between 330 and 390 K, the binding energy and the intensity of the N 1s peak at 399.5 eV remain unchanged, whereas the corresponding C 1s peak shows a further increase and a decreasing high-energy shoulder; this behavior is indicative of a further stepwise dehydrogenation in that temperature range. The fact that this further progressing reaction does not lead to changes in the N 1s region indicates that the pyrrole-ring-structure in NEC is not affected. This can be understood best, if also the β -hydrogen atoms of the pyrrole ring are rapidly abstracted in the initial dehydrogenation phase, leading to H₈-NEC as a first observable intermediate. H₈-NEC was also found as stable intermediate in other dehydrogenation experiments.^[19–21] The further stepwise dehydrogenation is supported by the fact that the H₁₂-NEC signal vanishes already at 350 K in the N 1s region, whereas it is observed up to 380 K in the C 1s region as the mentioned high-energy shoulder. This slower decrease of the “H₁₂-NEC” C 1s peak at 285.2 eV can be understood if one assigns this peak mainly to the CH₂ subunits in H_x-NEC and the peak at 284.5 eV mainly to CH subunits of H_x-NEC. Then the observed behavior is due to the progressive dehydrogenation of H₈-NEC to NEC. As mentioned above, the absence of changes in the N 1s signal between 330 and 390 K indicates that the local geometry of the pyrrole subunit (with the dehydrogenated α -

and β - carbon atoms) does not change as the other carbon atoms in the six-membered carbon rings are successively dehydrogenated to finally yield NEC. Direct evidence for NEC as the final product at 380 K comes from a comparison of the C 1s spectra from the heating series of H₁₂-NEC to spectra obtained for the direct adsorption of NEC on Pt(111) at low temperatures (see the Supporting Information). These spectra are in very good agreement, within the margin of error, indicating that this species is indeed NEC.

Starting at 390 K, further pronounced changes are observed. In the N 1s region a new peak develops at 398.1 eV, at the cost of the peak at 399.5 eV, and in the C 1s region a more gradual shift from 284.5 to 283.8 eV is observed. These changes are assigned to the unwanted dealkylation of NEC to carbazole, which in a technical process would modify the properties of the LOHC system in an undesired way, for example, due to the higher melting point of carbazole in comparison to NEC. While the N 1s peak shows a strong increase in intensity reaching a maximum at approximately 450 K, the corresponding C 1s peak intensity increases at a much slower pace. This is attributed to the fact that the dealkylation directly influences the nitrogen atom, whereas the carbon atoms in the benzene rings are affected to a much lesser extent. As there only is one nitrogen atom, the signal directly reflects the chemical environment. In contrast, there is a large number of non-equivalent carbon atoms. Thus only gradual shifts and a significant peak broadening are observed in the transition region, making the assignment of signals to surface species difficult. At even higher temperatures, up to 1000 K, further dehydrogenation and the formation of carbon and carbon fragments is occurring (data not shown).

In conclusion, we have derived a detailed understanding of the reaction behavior of a large liquid organic hydrogen carrier molecule on an atomically well-defined Pt(111) single crystal surface, which serves as model for the (111) facets of catalyst particles. In situ XPS during adsorption and while heating yields quantitative insights into the surface reaction in an unprecedented fashion, as is summarized in Scheme 1: As first reaction step, desorption of the H₁₂-NEC multilayers is observed, leaving a monolayer of H₁₂-NEC. H₁₂-NEC starts to dehydrogenate at 200 K, forming H₈-NEC as the first stable surface intermediate at approximately 330 K. The latter dehydrogenates to



Scheme 1. Reaction Scheme of H₁₂-NEC on a Pt(111) surface.

NEC until 380 K, whereas the detrimental reactions that form either carbazole or carbon fragments on the surface occur at temperatures above 390 K. The unloading reaction starts with the hydrogen atoms at the α - and β -carbon atoms in the pyrrole ring, whereas the outer benzene entities lose their hydrogen atoms at higher temperatures. Our study illustrates that in a certain temperature range H_{12} -NEC indeed is a regenerable hydrogen carrier molecule, with an optimal dehydrogenation temperature around 380 K under the conditions of a surface science experiment. We expect that the obtained mechanistic understanding of our model system will be extremely beneficial for the design and understanding of catalysts for LOHCs on a knowledge-driven basis.

Experimental Section

The experiments were conducted at the synchrotron BESSY II at beamline U 49/2 PGM 1 using a transportable two chamber ultra-high vacuum (UHV) setup.^[22] The preparation chamber houses typical surface science preparation and analysis tools such as a sputter gun, low energy electron diffraction (LEED), and dosing facilities. The main chamber is equipped with the electron energy analyzer and several dosing facilities, including a supersonic molecular beam and a dedicated dosing unit for the adsorption of H_{12} -NEC and NEC. The manipulator allows to cool the Pt(111) crystal to about 120 K by using liquid nitrogen; through direct heating sample temperatures of up to 1400 K can be reached. Additionally a filament is installed in the back of the sample that allows heating the sample while measuring without any disturbing effects. During adsorption or heating the sample, XP spectra in the region of interest can be obtained continuously, with typically 10 s per spectrum. The coverage was calibrated by comparison to known surface coverage, that is, the $c(4\times 2)$ CO superstructure on the Pt(111) surface for carbon atoms.^[23] For peak fitting in the N1s spectra we used a Doniach–Sunjic function to represent the peak shape after subtraction of the background. In the C1s spectra we used envelopes that represent the surface species; see for example Reference [24]. These envelopes consisted of two Doniach–Sunjic functions for one species, such as H_{12} -NEC and NEC, and of only one for CO and carbon fragments at higher temperatures, see the Supporting Information. Please note that the amount of CO on the surface during the experiments was below 0.1 ML. CO did not participate in the reaction and desorbed until 410 K, see Figure 2.

NEC was purchased in a sulfur-free quality (S-content < 50 ppm) from Hydrogenious Technologies GmbH (www.hydrogenious.net), whereas H_{12} -NEC was synthesized by hydrogenation of NEC using a Ru/AlOx catalyst (Alfa Aesar, 5 wt% Ru on support, 1 mol%) by reacting NEC (0.1 mol, 19.5 g) in cyclohexane (150 mL) under 50 bar hydrogen and 150 °C for 2 h.^[23]

Acknowledgements

We acknowledge the Cluster of Excellence “Engineering of Advanced Materials” and the BMW group for financial support. S.S. gratefully acknowledges a grant of the Fonds der Chemischen Industrie. BESSY staff is acknowledged for support during

beamtime. P.W. acknowledges the European Research Council (ERC) for supporting his fundamental work on the catalytic dehydrogenation of LOHC systems.

Keywords: dehydrogenation • hydrogen storage • liquid organic hydrogen carriers • photoelectron spectroscopy • surface reactions

- [1] U. Eberle, M. Felderhoff, F. Schüth, *Angew. Chem.* **2009**, *121*, 6732–6757; *Angew. Chem. Int. Ed.* **2009**, *48*, 6608–6630.
- [2] B. Müller, W. Arlt, P. Wasserscheid, *Energy Environ. Sci.* **2011**, *4*, 4322–4331.
- [3] S. Satyapal, J. Petrovic, C. Read, G. Thomas, G. Ordaz, *Catal. Today* **2007**, *120*, 246–256.
- [4] A. Haryanto, S. Fernando, N. Murali, S. Adhikari, *Energy Fuels* **2005**, *19*, 2098–2106.
- [5] B. Sakintuna, F. Lamari-Darkrim, M. Hirscher, *Int. J. Hydrogen Energy* **2007**, *32*, 1121–1140.
- [6] D. Teichmann, W. Arlt, P. Wasserscheid, R. Freymann, *Energy Environ. Sci.* **2011**, *4*, 2767–2773.
- [7] D. Teichmann, K. Stark, K. Müller, G. Zottl, P. Wasserscheid, W. Arlt, *Energy Environ. Sci.* **2012**, *5*, 9044–9054.
- [8] K. M. Eblagon, D. Rentsch, O. Friedrichs, A. Remhof, A. Zuetzel, A. J. Ramirez-Cuesta, S. C. Tsang, *Int. J. Hydrogen Energy* **2010**, *35*, 11609–11621.
- [9] K. M. Eblagon, K. Tam, K. M. K. Yu, S.-L. Zhao, X.-Q. Gong, H. He, L. Ye, L.-C. Wang, A. J. Ramirez-Cuesta, S. C. E. Tsang, *J. Phys. Chem. C* **2010**, *114*, 9720–9730.
- [10] G. P. Pez, A. R. Scott, A. C. Cooper, H. Cheng (Air Products and Chemicals Inc.), US Patent US7 101 530 B2, **2006**.
- [11] F. Sotoodeh, L. Zhao, K. J. Smith, *Appl. Catal. A* **2009**, *362*, 155–162.
- [12] W. Liu, A. Savara, X. Ren, W. Ludwig, K.-H. Dostert, S. Schaueremann, A. Tkatchenko, H.-J. Freund, M. Scheffler, *J. Phys. Chem. Lett.* **2012**, *3*, 582–586.
- [13] F. Sotoodeh, K. J. Smith, *J. Phys. Chem. C* **2013**, *117*, 194–204.
- [14] M. Sobota, I. Nikiforidis, M. Amende, B. S. Zanón, T. Staudt, O. Höfert, Y. Lykhach, C. Papp, W. Hieringer, M. Laurin, D. Assenbaum, P. Wasserscheid, H.-P. Steinrück, A. Görling, J. Libuda, *Chem. Eur. J.* **2011**, *17*, 11542–11552.
- [15] C. Papp, T. Fuhrmann, B. Tränkenschuh, R. Denecke, H. P. Steinrück, *Phys. Rev. B* **2006**, *73*, 235426.
- [16] T. Fuhrmann, M. Kinne, B. Tränkenschuh, C. Papp, J. F. Zhu, R. Denecke, H.-P. Steinrück, *New J. Phys.* **2005**, *7*, 107.
- [17] C. Papp, R. Denecke, H. P. Steinrück, *Langmuir* **2007**, *23*, 5541–5547.
- [18] N. Luckas, K. Gotterbarm, R. Streber, M. P. A. Lorenz, O. Höfert, F. Vines, C. Papp, A. Görling, H.-P. Steinrück, *Phys. Chem. Chem. Phys.* **2011**, *13*, 16227–16235.
- [19] F. Sotoodeh, B. J. M. Huber, K. J. Smith, *Appl. Catal. A* **2012**, *419–420*, 67–72.
- [20] Z. Wang, I. Tonks, J. Belli, C. M. Jensen, *J. Organomet. Chem.* **2009**, *694*, 2854–2857.
- [21] M. Yang, C. Han, G. Ni, J. Wu, H. Cheng, *Int. J. Hydrogen Technol.* **2012**, *37*, 12839–12845.
- [22] R. Denecke, M. Kinne, C. M. Whelan, H.-P. Steinrück, *Surf. Rev. Lett.* **2002**, *9*, 797.
- [23] J. S. McEwen, S. H. Payne, H. J. Kreuzer, M. Kinne, R. Denecke, H. P. Steinrück, *Surf. Sci.* **2003**, *545*, 47–69.
- [24] C. Papp, B. Tränkenschuh, R. Streber, T. Fuhrmann, R. Denecke, H. P. Steinrück, *J. Phys. Chem. C* **2007**, *111*, 2177–2184.

Received: March 25, 2013

Published online on May 14, 2013